


**Backpropagated frame transformation theory: A reformulation**

Dávid Hvizdoš

*J. Heyrovský Institute of Physical Chemistry, ASCR, Dolejškova 3, 18223 Prague, Czech Republic  
and Institute of Theoretical Physics, Faculty of Mathematics and Physics, Charles University in Prague,  
V Holešovičkách 2, 18000 Prague, Czech Republic*

Chris H. Greene

*Department of Physics and Astronomy, Purdue University, West Lafayette, Indiana 47907, USA  
and Purdue Quantum Science and Engineering Institute, Purdue University, West Lafayette, Indiana 47907, USA*Roman Čurík *J. Heyrovský Institute of Physical Chemistry, ASCR, Dolejškova 3, 18223 Prague, Czech Republic*

(Received 7 October 2019; revised manuscript received 5 December 2019; published 28 January 2020)

The energy-dependent frame transformation theory of Gao and Greene [H. Gao and C. H. Greene, *Phys. Rev. A* **42**, 6946 (1990)] is extended to yield a quantitatively accurate description of the dissociative recombination process. Evidence is presented to show that direct application of the original theory leads to inaccurate cross sections. A major revision, based on an interaction-free backpropagation of the Born-Oppenheimer solutions, markedly improves the frame transformation theory, reducing its average error by orders of magnitude. The original theory and its extension are tested on the previously explored two-dimensional (2D) model that is tailored to describe the singlet ungerade states of molecular hydrogen. The 2D model can be solved exactly (within the numerical accuracy) without implementing the Born-Oppenheimer approximation. These exact results then serve as a benchmark for the frame transformation theory developed in this paper.

DOI: [10.1103/PhysRevA.101.012709](https://doi.org/10.1103/PhysRevA.101.012709)**I. INTRODUCTION**

Rovibrational frame transformation (FT) theory [1] divides the electronic space into two parts: the inner (body frame) and the outer (laboratory frame) regions. Electronic and nuclear Hamiltonians are considered decoupled in the outer region and hence the solutions of the outer-region Schrödinger equation are linear combinations of products of the electronic and rovibrational wave functions. Solutions of the system in the inner region are assumed to be quasiseparable Born-Oppenheimer wave functions. The role of the frame transformation theory is to smoothly connect the independent solutions in these two regions.

In treatments of inelastic collisions between electrons and neutral molecules the adiabatic-nuclei approximation [2] has often been assumed [3–5]. Formally this technique can be viewed as an application of the FT procedure carried out at infinite electronic radius. Therefore, the FT theory should not be confused with the adiabatic-nuclei approximation, as the former exploits the Born-Oppenheimer approximation (BOA) only at small electronic distances, while the latter employs it over the entire electronic space.

Combinations of the FT approach with multichannel quantum defect theory (MQDT) [6,7] have been previously applied to treat numerous electron-cation collision and molecular photofragmentation systems (see, e.g., Refs. [8–17]) and still

more applications can be found in Rydberg spectroscopy [7]. The cornerstone of these studies is the body-frame quantum defect (or phase shift)  $\mu(R, \epsilon)$  that describes a phase gained by the scattered (or Rydberg) electron inside the molecular core. The difficulty in application of the FT theory has always been in the choice of the body-frame energy  $\epsilon$  at which the quantum defect  $\mu(R, \epsilon)$  is determined. This crucial question needs to be addressed in order to calculate vibrational matrix elements of operators such as  $\sin \pi \mu(R, \epsilon)$  and  $\cos \pi \mu(R, \epsilon)$ . This problem does not arise in cases where the energy dependence of  $\mu$  can be neglected, as in the vast majority of the MQDT studies carried out up to this date. However, two different theoretical approaches were developed to account for the energy dependence of the inner solutions. A common element of these two treatments is the introduction of the electron-molecule compound potential-energy curves, along which the nuclei move when the scattered electron is inside the inner region. Unlike the bound-state problems, where the BOA potential-energy curves are well defined, for the continuum electronic energies there is not an obvious *a priori* way to connect electronic BOA energies at nuclear coordinates  $R$  with those determined at  $R + \delta$ . This has led to development of the two different FT theories that differ in their choices of the BOA potential-energy curves.

In the first approach [18] (further extended in Refs. [19,20]), the potential-energy curves in the continuum were chosen such that the quantum defect  $\mu(R, \epsilon)$  does not depend on the internuclear distance  $R$ . The difficulty of this method lies in finding these potential-energy curves.

\*roman.curik@jh-inst.cas.cz

Once they are known, the frame transformation matrix can be reduced, in this case, only to a Franck-Condon overlap integral between the vibrational states of the target and those of the compound [18].

In the second approach [21], the compound BOA potential-energy curves are chosen explicitly as curves parallel to the curve of the target molecular system. The vertical distance of the compound curves from the target curve correlates with the collision energy of the electron in the incident vibrational channel. The method was successfully tested for resonant electron-impact vibrational excitation of  $N_2$  and for determination of vibrational levels of the  $H_2 B''$  state. However, there has been no application to dissociative recombination.

In the present study we adopt the second approach to study indirect dissociative recombination with energy-dependent frame transformation theory. Part of our motivation for this choice lies in the similarity between the compound bound potential-energy curves (Rydberg curves) and the target cation curve. In order to assess the results, the approximate FT theory is applied to a model two-dimensional (2D) system [22] tailored to describe dissociative recombination of  $H_2^+$  through its singlet ungerade channels. This 2D model can be solved exactly (within numerical accuracy) [22,23], which bypasses all physical approximations and thus serves as an exact benchmark for the approximate FT theory.

## II. ENERGY-DEPENDENT FRAME TRANSFORMATION

In this section we briefly summarize the basic steps of the energy-dependent FT of Ref. [21] applied to the 2D model. This theory is the starting point of the present study.

The 2D model has two different modes of fragmentation associated with the competing dissociation and ionization (or detachment) channels and is described by the Schrödinger equation

$$[H_n(R) + H_e(r) + V(R, r) - E]\psi(R, r) = 0, \quad (1)$$

where

$$H_n(R) = -\frac{1}{2M} \frac{\partial^2}{\partial R^2} + V_0(R), \quad (2)$$

$$H_e(r) = -\frac{1}{2} \frac{\partial^2}{\partial r^2} + \frac{l(l+1)}{2r^2} - \frac{1}{r}. \quad (3)$$

The potential curve  $V_0(R)$  describes the vibrational motion of the target molecule. The potential-energy function  $V(R, r)$  couples the electronic and nuclear degrees of freedom and is set to approximately describe the singlet ungerade Rydberg series of  $H_2$  and the singlet ungerade low-energy scattering of electrons by  $H_2^+$ . More details and the exact forms of the potentials  $V_0(R)$  and  $V(R, r)$  can be found in Refs. [22,23].

The goal of the frame transformation theory is to obtain the scattering (or reactance) matrix describing the coupling of asymptotic channels at all distances beyond some fixed electronic radius  $r_0$ . A set of linearly independent Born-Oppenheimer solutions to Eq. (1) can be written in the inner region for  $r < r_0$  as

$$\psi_{i'}(R, r) = \phi_{i'}(R) F_{i'}(R; r), \quad (4)$$

where  $\phi_{i'}(R)$  are vibrational eigensolutions of the target (or compound) nuclear Hamiltonian (2) with eigenenergies  $E_{i'}$ .

The electronic solutions  $F_{i'}(R; r)$  are normalized electronic BOA eigensolutions at the fixed coordinate  $R$  with eigenenergies  $\epsilon_{i'}$ . The total energy is  $E = E_{i'} + \epsilon_{i'}$ . Note that the energy spectrum of the BOA solutions (4) is continuous since no boundary condition was applied at  $r = r_0$ . The distance  $r_0$  is chosen as small as possible to ensure validity of the Born-Oppenheimer approximation inside the electronic volume confined by  $r_0$ . On the other hand, the present model Hamiltonian  $H$  has no long-range power-law potential coupling terms, and the chosen value  $r_0$  is also such that for  $r \geq r_0$  all the interaction terms in  $H$  apart from the Coulomb potential are negligible.

As is standard in quantum defect treatments, for  $r \geq r_0$  the interaction with the molecular core is assumed to be solely the Coulomb potential. This allows us to write the electronic inner-region Born-Oppenheimer solutions at  $r_0$  as

$$F_{i'}(R; r_0) = N(R, \epsilon_{i'}) [f_{\epsilon_{i'}}(r_0) \cos \pi \mu(R, \epsilon_{i'}) - g_{\epsilon_{i'}}(r_0) \sin \pi \mu(R, \epsilon_{i'})]. \quad (5)$$

Here  $f_{\epsilon_{i'}}(r_0) \equiv f_{i'}(r_0)$  and  $g_{\epsilon_{i'}}(r_0) \equiv g_{i'}(r_0)$  are regular and irregular Coulomb functions evaluated for the energy  $\epsilon_{i'}$ . The normalization factor  $N(R, \epsilon_{i'})$  was introduced to ensure the volume normalization of  $F_{i'}(R; r)$ , since the term in brackets is just a surface term not possessing any kind of normalization. It has been shown previously [19,24] that the normalization factor can be evaluated solely from the surface properties as

$$N(R, \epsilon) = \left[ \frac{\partial \mu(R, \epsilon)}{\partial \epsilon} + \frac{1}{2} W(R, \epsilon) \right]^{-1/2}, \quad (6)$$

with

$$W(R, \epsilon) = ([f_\epsilon, g'_\epsilon] + [g_\epsilon, f'_\epsilon]) \sin \pi \mu(R, \epsilon) \cos \pi \mu(R, \epsilon) - [f_\epsilon, f'_\epsilon] \cos^2 \pi \mu(R, \epsilon) - [g_\epsilon, g'_\epsilon] \sin^2 \pi \mu(R, \epsilon), \quad (7)$$

where  $[f, g]$  denotes the Wronskian of functions  $f$  and  $g$ , and  $f' \equiv \partial f / \partial \epsilon$ .

In the outer region ( $r > r_0$ ) the independent solutions (4) can be written as a linear combination of channel functions (close-coupling expansion):

$$\psi_{i'}(R, r) = \sum_i \phi_i(R) [f_i(r) I_{ii'} - g_i(r) J_{ii'}]. \quad (8)$$

Matching of Eqs. (4) and (8) at  $r_0$  determines the matrices

$$\begin{aligned} I_{ii'} &= [f_{i'}, g_i] C_{ii'} - [g_{i'}, g_i] S_{ii'}, \\ J_{ii'} &= [f_{i'}, f_i] C_{ii'} - [g_{i'}, f_i] S_{ii'}, \end{aligned} \quad (9)$$

with

$$\begin{aligned} C_{ii'} &= \int dR \phi_i(R) N(R, \epsilon_{i'}) \cos \pi \mu(R, \epsilon_{i'}) \phi_{i'}(R), \\ S_{ii'} &= \int dR \phi_i(R) N(R, \epsilon_{i'}) \sin \pi \mu(R, \epsilon_{i'}) \phi_{i'}(R). \end{aligned} \quad (10)$$

The short-range  $K$  matrix is then obtained as  $\underline{K} = \underline{J} \underline{I}^{-1}$ .

In a manner similar to our previous studies [11,14,17,25,26], instead of real vibrational functions, we employ a complex vibrational basis  $\phi_i(R)$ . Such a basis can be obtained by applying the Siegert boundary condition [27–29]

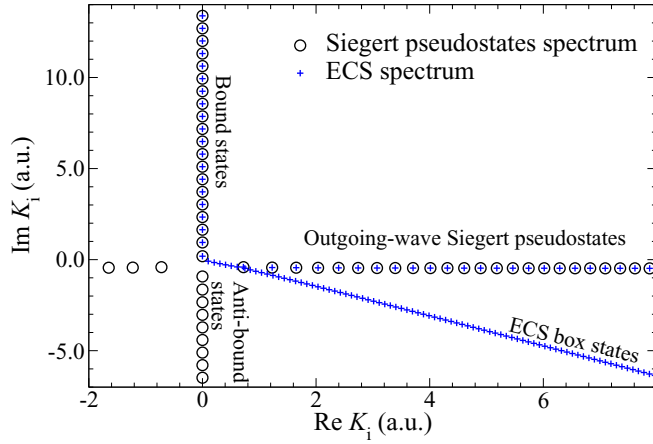


FIG. 1. Distribution of the Siegert pseudostate poles (circles) defined by  $R_0 = 15$  bohr and of the ECS poles with the complex contour (11) (crosses) in the complex nuclear momentum plane.

at the nuclear coordinate  $R = R_0$  or, as is done in the present study, by solving the nuclear Schrödinger equation along a contour  $Z$  in the complex plane. The zero-value boundary condition is applied here at both ends of the contour. We utilize the technique of exterior complex scaling (ECS) [30,31] with the complex contour chosen as

$$Z = \begin{cases} R, & \text{for } R \leq R_0, \\ R_0 + e^{i\theta}(R - R_0), & \text{for } R_0 < R \leq R_m, \end{cases} \quad (11)$$

where  $R$  is a real parameter along the complex contour  $Z$ ,  $R_0 = 15$  bohr denotes the bending point,  $\theta = 40^\circ$  is the bending angle, and  $R_m = 40$  bohr parametrizes the final point  $Z_m$  of the complex contour. The spectra of the Siegert and ECS systems are similar, as is shown in Fig. 1. The ECS spectrum contains two branches coinciding with the bound states and outgoing-wave Siegert pseudostates, while it is missing branches with the antibond states and incoming-wave Siegert pseudostates. The linear branch close to negative  $40^\circ$  corresponds to ECS states defined by the zero boundary condition at the end of the bent interval. Note that the coincidence of the outgoing-wave Siegert spectrum and the ECS spectrum is due to the coincidence of the Siegert boundary  $R_0$  with the bending point of the ECS contour (11).

The resulting cross section obtained with the selected subset of Siegert states [22] and those obtained with the ECS states are numerically equal except for some small-energy windows, at which high sensitivity to the completeness of the vibrational basis can be observed. Our experience shows that the ECS states are complete to better numerical accuracy, when compared to the completeness of the bound states and outgoing-wave subset of Siegert pseudostates.

Completeness of the vibrational basis also affects the symmetry of the resulting  $K$  matrix. The symmetry of the  $K$  matrix is also further disturbed by the right-index dependence of the body-frame energy  $\epsilon$  in Eqs. (10). We have observed that the symmetry of the short-range  $K$  matrix is essential for stability of the final cross sections. Therefore, in the present study the  $K$  matrix is artificially symmetrized by the replacement  $K \rightarrow (K + K^T)/2$  before the closed channels are eliminated in the MQDT calculation. A similar ad hoc symmetrization step was

also reported as being necessary in a previous application of the energy-dependent FT theory to dissociative electron attachment of electrons colliding with  $H_2$  [20]. It is important to note that in the ECS (or Siegert pseudostates) basis the  $K$  matrix should not be expected to be Hermitian, owing to the missing complex conjugate of  $\phi_i(R)$  in Eq. (10).

After the Cayley transformation of the short-range  $K$  matrix to the short-range  $S$  matrix

$$\underline{S} = (\underline{1} + i\underline{K})(\underline{1} - i\underline{K})^{-1}, \quad (12)$$

the physical  $S$  matrix is obtained by the standard closed-channel elimination technique of the MQDT:

$$\underline{S}^{\text{phys}} = \underline{S}^{oo} - \underline{S}^{oc}[\underline{S}^{cc} - e^{-2i\beta(E)}]^{-1}\underline{S}^{co}, \quad (13)$$

where the superscripts  $o$  and  $c$  denote open and closed subblocks in the short-range  $S$  matrix, respectively. Whether a channel is open or closed is determined by the real part of its complex energy. The diagonal matrix  $\underline{\beta}(E)$  describes effective Rydberg quantum numbers with respect to the closed-channel thresholds  $E_i$ :

$$\beta_{ij} = \frac{\pi}{\sqrt{2(E_i - E)}}\delta_{ij}. \quad (14)$$

Finally, the utilization of the complex nuclear basis with the outgoing-wave boundary conditions at  $R_0$  allows us to compute the dissociative flux solely on the electronic surface. The defect of unitarity of the electronic physical  $S$  matrix  $\underline{S}^{\text{phys}}$ , i.e., the missing electronic flux of the system, can be identified [11] with the dissociative flux

$$\sigma_{i'}(\epsilon_{i'}) = \frac{\pi}{2\epsilon_{i'}} \left[ 1 - \sum_i S_{i'i}^{\text{phys}\dagger} S_{i'i}^{\text{phys}} \right]. \quad (15)$$

The validity of this ansatz was previously confirmed using the 2D model [22]. This approach does have one important limitation, in that it is unable to separate the partial dissociative recombination (DR) cross sections in different dissociation channels, because the method computes only the total dissociative flux.

### III. APPLICATION OF THE FT THEORY TO THE 2D MODEL

We employ the energy-dependent frame transformation theory presented in the previous section to calculate the dissociative recombination cross sections for the 2D model.

This direct implementation leads to inaccurate resonance line shapes and cross-section magnitudes, as is shown in Fig. 2. The essentially exact solution represented by the black curve was obtained with the 2D  $R$ -matrix method [23], while the red dashed curve represents results obtained with the energy-dependent FT of Ref. [21] in the form that is summarized above and extended to treat the dissociative process in this work. The frame transformation radius was set at the value  $r_0 = 7$  bohr radii, chosen here as the shortest possible distance beyond which the electron-cation interaction  $V(R, r_0)$  can be neglected. Figure 2 shows the comparison in the energy window 0–0.5 eV, but the disagreement is very similar throughout the entire interval we have computed: 0–2 eV.

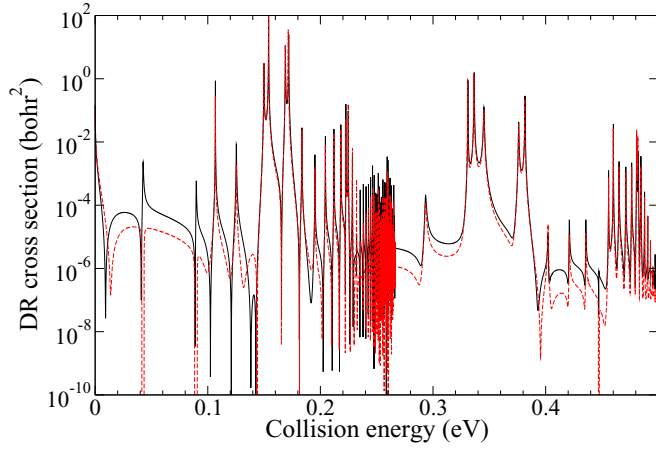


FIG. 2. DR cross sections obtained from the exact solution of the 2D Hamiltonian (solid line) and from the direct application of the present extension (with ECS in place of Siegert states as summarized in Sec. II) of the energy-dependent FT theory [21] (dashed line).

One of our previous publications [23] indicated that the reason for the failure of the energy-dependent FT theory applied to the DR can be connected with inaccuracy of the Born-Oppenheimer approximation inside the sphere confined by  $r_0 = 7$  bohr. Figure 3 displays the real part of the energy levels of all the 120 target ion states included in the present study, for which the Born-Oppenheimer approximations (4) and (5) are assumed by the FT theory. Figure 3 also shows, as the thick horizontal line, the energy of the nuclei after their dissociation into the  $n = 2$  channel, triggered by zero-energy incident electrons. The high density of states at low positive energies is caused by the chosen bending angle  $\theta = 40^\circ$  and by the large value of  $R_0$  of the complex contour for generation of the ECS basis. Figure 3 is helpful to indicate

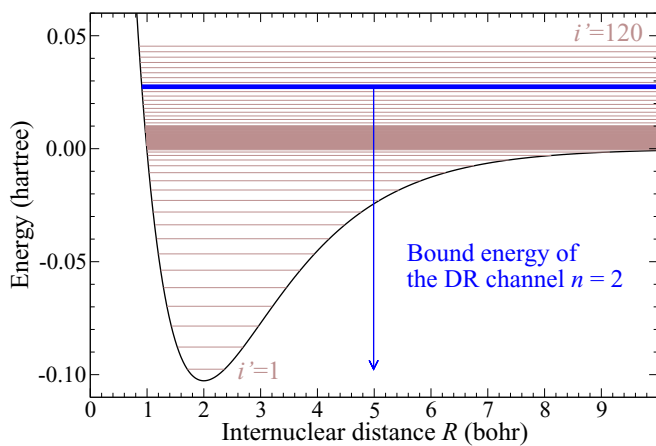


FIG. 3. The potential energy of the target cation is plotted versus the coordinate  $R$  of the model Hamiltonian. Real parts of the vibrational energies of the nuclear functions  $\phi_i(R)$  are displayed as horizontal lines. The length of the vertical arrow displays the binding energy (close to  $-1/8$  Hartree) of one of the outgoing atomic fragments in its  $n = 2$  state. The thick horizontal line is the kinetic energy of the nuclei in the  $n = 2$  DR channel for zero incident electron energy.

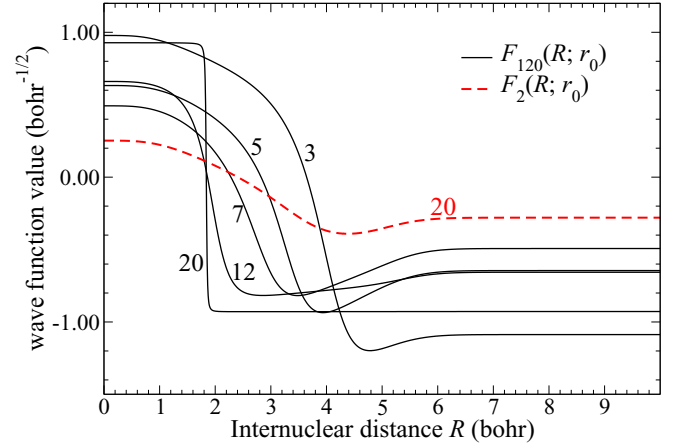


FIG. 4. Shape of the electronic wave function  $F_i(r_0; R)$  defined by Eq. (5) on the electronic surface  $r_0$  for the following radii:  $r_0 = 3, 5, 7, 12,$  and  $20$  bohr. The electronic energy corresponds to  $i' = 120$  for black curves and  $i' = 2$  for the dashed curve.

the minimum number of ECS nuclear states that are needed by these calculations in order to describe dissociation into the  $n = 2$  state in the  $0$ – $0.5$  eV incident collision energy window.

Validity of the BOA for the neutral complex in the present theory is connected with the size of  $\partial F_i(R; r_0)/\partial R$  for all the states included. Qualitatively, one can assess its accuracy by inspecting the functions  $F_i(R; r_0)$  displayed in Fig. 4 for the highest  $i' = 120$  state included and for different electronic radii  $r_0$ . As can be seen, as the electronic radius  $r_0$  increases, the wave function  $F_{120}(R; r_0)$  changes from positive to negative value over a smaller  $R$  interval, generating a large magnitude of  $\partial F_i(R; r_0)/\partial R$  on the surface  $r_0$ . The situation is less critical for lower states, e.g., the dashed line shows  $F_2(R; r_0)$  at  $r_0 = 20$  bohr. Thus good accuracy of the BOA inside even fairly large electronic sphere radii can be expected for vibrational excitation studies. However, once the relevant dissociative channels are included, the BOA leads to inaccurate results already at  $r_0 = 7$  bohr in the present study. Note that surface values of  $F_{120}(R; r_0)$  for  $r_0 = 3$  and  $5$  bohr are computed inside the electron-cation interaction and the wave function cannot be considered to reside in the asymptotic electronic region.

#### IV. BACKPROPAGATED FRAME TRANSFORMATION

Breakdown of the Bohr-Oppenheimer approximation, shown for the dissociative nuclear wave functions, leads to a question as to whether it is possible to decrease the frame transformation radius  $r_0$  to unphysically small values while still keeping all the information about the electron-cation interaction. Such a procedure is indeed possible and has been designed here to consist of the three following steps:

(i) Determination of the energy-dependent quantum defect  $\mu(R, \epsilon)$  at an appropriate electronic radius at which the quantum defect is stable and converged, containing all the phase shift relative to the Coulomb plus centrifugal potential which is acquired in the electron-cation interaction. In the present study this value is approximately  $r_0 \geq 7$  bohr. Knowledge

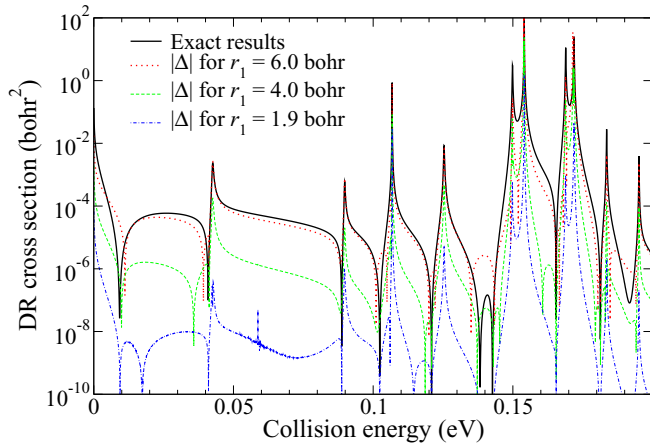


FIG. 5. DR cross sections for different backpropagation distances. The thick line shows the absolute exact results. Remaining data (denoted by the symbol  $|\Delta|$ ) show absolute values of a difference between the backpropagated results and the exact results. The backpropagation distances were  $r_1 = 6.0$  bohr (dotted line), 4.0 bohr (dashed line), and 1.9 bohr (dot-dashed line).

of the fixed- $R$  quantum defect allows us to write the BOA solution  $F(R; r)$  in Eq. (5) for  $r > r_0$ .

(ii) Backpropagation of the electronic BOA solution  $F(R; r)$  in the Coulomb field only to small distances  $r_1$ , while ignoring the electron-molecule interaction  $V(R, r)$ , even though it is clearly non-negligible at the small distance  $r_1$ .

(iii) The energy-dependent frame transformation of the backpropagated solutions at  $r_1$  then proceeds as is described in Sec. II.

This proposed procedure is very simple to implement in practice. Once the full  $\mu(R, \epsilon)$  is determined, the backpropagation of the electronic BOA functions (5) is implemented by a simple evaluation of the Coulomb functions  $f_{i'}^l$  and  $g_{i'}^l$  at smaller different electronic radius  $r_1$ . Both steps (i) and (ii) are executed simply by replacing  $r_0$  in Eqs. (5)–(9) with  $r_1 < r_0$ . In cases where  $\partial\mu(R, \epsilon)/\partial\epsilon > 0$ , the radius  $r_1$  can even be pushed to zero. In the present case,  $\partial\mu(R, \epsilon)/\partial\epsilon$  is negative and there is a bottom limit of  $r_1 = 1.9$  bohr below which the BOA wave function  $F(R; r)$  becomes difficult to normalize with Eq. (6) as the term in brackets becomes negative for some  $R$  values. This minimum value of  $r_1 \sim 1.9$  bohr also is reasonable, in view of the fact that the Coulomb plus centrifugal potential for  $l = 1$  reaches its minimum value at  $r = 2$  bohr.

In order to quantitatively test this ad hoc procedure we have applied it to the 2D model problem. The Born-Oppenheimer wave functions  $F(R; r)$  obtained at  $r = r_0 = 7.0$  bohr were backpropagated to three different distances:  $r_1 = 6.0, 4.0$ , and 1.9 bohr radii. Absolute values of the difference between the backpropagated results and the exact results (denoted as  $|\Delta|$ ), together with the exact cross sections, are shown in Fig. 5. The data demonstrate that the backpropagation step remarkably improves the FT results. Backpropagation results for  $r_1 = 1.9$  bohr are within 0.1% of the exact cross sections. For clarity the comparisons are presented over a narrower energy window of 0–0.2 eV, but our presented conclusions remain valid over the entire region examined: 0–2 eV.

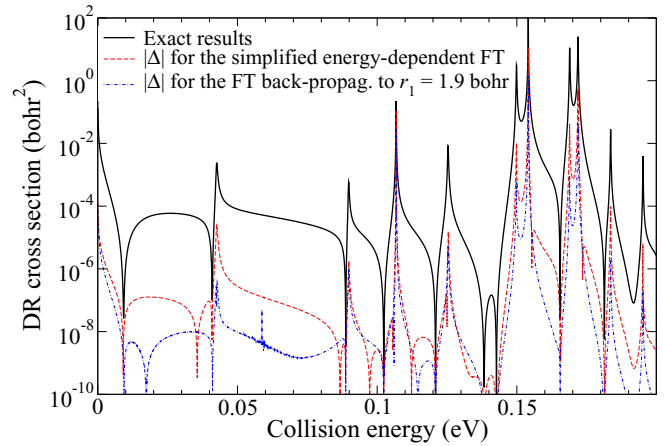


FIG. 6. DR cross sections for different backpropagation models. The solid curve shows the absolute exact results. Data obtained by the backpropagated FT ( $r_1 = 1.9$  bohr) are shown as a dot-dashed curve, while the results of the simplified energy-dependent FT are displayed as a dashed curve. Both FT data sets display absolute values of their difference from the exact results, as denoted by the symbol  $|\Delta|$ .

### A. Simplified version

A simplified version of the backpropagation procedure is based on properties of the Coulomb functions  $f_\epsilon(r)$  and  $g_\epsilon(r)$ , which lose their energy dependence as  $r$  approaches zero value. In this limit it is reasonable to assume that Eq. (9) simplifies to

$$I_{i'v} = C_{i'v}, \quad J_{i'v} = S_{i'v}, \quad (16)$$

and thus  $\underline{K} = \underline{S}\underline{C}^{-1}$ . The normalization factor  $N(R, \epsilon)$  (6) approaches high values as the backpropagation radius  $r_1$  is pushed to the limit. This limit is  $r_1 \rightarrow 0$  for  $\partial\mu(R, \epsilon)/\partial\epsilon > 0$  or some small finite value for  $\partial\mu(R, \epsilon)/\partial\epsilon < 0$ . The normalization factor does not exactly cancel out in the  $\underline{S}\underline{C}^{-1}$  product due to right-index dependence of its energy argument in Eqs. (10). However, if the cancellation of  $N(R, \epsilon)$  is assumed by

$$C_{i'v} = \int dR \phi_i(R) \cos \pi \mu(R, \epsilon_{i'}) \phi_{i'}(R),$$

$$S_{i'v} = \int dR \phi_i(R) \sin \pi \mu(R, \epsilon_{i'}) \phi_{i'}(R), \quad (17)$$

the evaluation of the normalization factor can be avoided. Moreover, the backpropagation radius  $r_1$  does not explicitly enter the simplified backpropagation procedure anymore. This simplified backpropagation procedure coincides with the simplified FT technique that was implemented in practice [21] for the resonant electron-impact vibrational excitation of  $N_2$  and for the determination of the vibrational levels of  $H_2$  in its  $B''^1\Sigma_u^+$  electronic state.

Figure 6 demonstrates that the simplification leads to a loss in accuracy of about 1 order of magnitude, when compared to the backpropagated FT. However, regardless of its simplicity, the simplified version, applied to the present model, yields results that are within 1% accuracy from the exact cross sections. It is also simpler to implement, in that it only requires

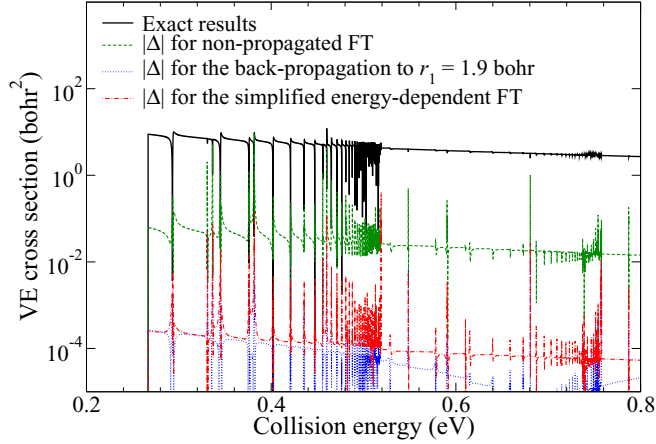


FIG. 7. Vibrational excitation cross sections for the transition  $0 \rightarrow 1$ . The solid curve shows the exact results. Data obtained by the energy-dependent frame transformation without the backpropagation are shown by the dashed line, and the results of the backpropagated FT ( $r_1 = 1.9$  bohr) are displayed by the dot-dashed curve. Cross sections for the simplified backpropagated FT are shown by the dash-dot curve. All three FT data sets display absolute values of their difference from the exact results, as denoted by the symbol  $|\Delta|$ .

knowledge of the body-frame quantum defect function and the vibrational wave functions, as the Coulomb functions  $f$  and  $g$  no longer appear in the integrals needed.

### B. Vibrational excitation

In the previous section it was demonstrated that the backpropagation technique leads to an improvement of the frame transformation theory for the dissociative recombination process. The frame transformation theory can also be applied for another collisional process that involves nuclear dynamics, namely vibrational excitation. The theoretical description of the vibrationally inelastic process also relies on the Born-Oppenheimer approximation inside the inner region, however, as is qualitatively demonstrated in Fig. 4, to a lesser extent. This is clearly visible in Fig. 7 which shows that no backpropagation is necessary to obtain 1% agreement between the energy-dependent FT theory and the exact results. However, also in the case of the vibrational excitation process, the backpropagation procedure leads to further improvement in the accuracy of the FT theory. Inaccuracies of the FT procedure are decreased by another 2 orders of magnitude, as is evident from Fig. 7. Note that the accuracies of the full backpropagation procedure and of its simplified version are comparable.

### C. Connection to the energy-independent approach

The reason for failure of the direct application of the energy-dependent FT theory [21] demonstrated at the start of Sec. III (Fig. 2) lies in a poor accuracy of the BOA solutions (4) within the electronic volume. The accuracy of these solutions degrades with increasing channel index  $i'$  and they lead to the inaccurate results shown in Fig. 2 once the channels above the thick blue line in Fig. 3 are included. Those channels are necessary to include for the DR process

but they are not needed for the vibrational excitation—only the collision process to which the energy-dependent FT [21] has been applied previously.

The simpler energy-independent frame transformation theory has historically been widely used to treat scattering problems ([12,32,33] and many other). Even its previous implementation for the 2D model [22] yielded more accurate results than the present direct application of the energy-dependent FT theory shown in Fig. 2. It is important to understand why the direct application of the energy-dependent FT theory worsens the DR cross section when compared to the previous energy-independent results [22].

The energy-independent FT theory, as implemented previously, does not neglect only the energy dependence of the quantum defect. It completely neglects the energy dependence of the BOA solutions (4) at  $r_0$  by additionally omitting the energy dependence of the Coulomb functions  $f_\epsilon(r_0)$  and  $g_\epsilon(r_0)$ . While the Coulomb functions lose their energy dependence in the limit  $r_0 \rightarrow 0$ , at distances of  $r_0 = 7$  bohr the change of the wave function (5) through the energy dependence of  $f_\epsilon(r_0)$  and  $g_\epsilon(r_0)$  is even larger than its change through the energy dependence of the quantum defect  $\mu(R, \epsilon)$  (for the present singlet ungerade  $H_2$  model).

Our presently proposed simplified backpropagation procedure (Sec. IV A) is based as well on omitting the energy dependence of the  $f_\epsilon$  and  $g_\epsilon$  functions at small electronic radii. An additional assumption of  $\partial\mu(R, \epsilon)/\partial\epsilon = 0$  makes it equivalent to the energy-independent approach because the normalization factor (6) cancels out exactly in the product of  $\underline{S}C^{-1}$ . The form (10) can be replaced by

$$\begin{aligned} C_{ii'} &= \int dR \phi_i(R) \cos \pi \mu(R) \phi_{i'}(R), \\ S_{ii'} &= \int dR \phi_i(R) \sin \pi \mu(R) \phi_{i'}(R). \end{aligned} \quad (18)$$

The fact that the frame transformation distance  $r_0$  is never evaluated in the energy-independent FT procedure can be viewed as a silent application of  $r_0 \rightarrow 0$  at which the energy dependence of the  $f_\epsilon$  and  $g_\epsilon$  functions diminishes. In summary, the generally good performance of the energy-independent FT theory, in the form that has been employed by many authors in recent decades, can be viewed as a result of the fact that it bypasses limitations of the Born-Oppenheimer approximation in a manner equivalent to the presented simplified backpropagation procedure.

## V. CONCLUSIONS

The present study describes an extension of the energy-dependent frame transformation theory by Gao and Greene [21] to dissociative recombination processes. The extension is achieved by use of the complex outgoing-wave-type nuclear basis, implemented here through exterior complex scaling of the nuclear Hamiltonian. Direct application of the method is shown to yield inaccurate results due to the limited validity of the Born-Oppenheimer approximation for the dissociative processes. The demonstration is carried out on a simple but realistic 2D model system tailored to describe the dissociative recombination of  $H_2^+$  through the singlet ungerade channels,

which is an example of the indirect dissociative recombination process. Since the 2D model can be solved exactly, to any desired numerical accuracy, its solutions provide an accurate benchmark to test the frame transformation theory.

An additional procedure, based on the interaction-free backpropagation of the BOA solutions, is proposed to improve validity of the BOA inside the frame transformation radius. This ad hoc technique leads to a remarkable improvement of the computed DR cross sections, reproducing the exact results within 0.1% accuracy. A simplified version of the backpropagation procedure is also presented as a trade-off between accuracy and simplicity. Accuracy of the simplified version is estimated to be within about 1% of the exact results.

The present study also qualitatively demonstrates that the vibrationally inelastic process is less sensitive to failure of the Born-Oppenheimer approximation in the inner region, because its description does not require such strongly closed channels as the ones that are necessary in the DR theory. Consequently, no backpropagation is needed for vibrational excitation cross-section calculations, provided 1% accuracy is viewed as sufficient. However, application of the backpropagation step improves the results, at least for the present model, by another 2 orders of magnitude in accuracy. In

the case of vibrational excitation, the full backpropagation technique and its simplified version perform similarly in terms of accuracy.

The backpropagation technique, proposed here, acts only on the electronic part of the Born-Oppenheimer wave function. Therefore we expect the procedure should be applicable to molecular systems with more nuclear degrees of freedom. Both sets of nuclear states, the Siegert pseudostates and the ECS states, can be employed in such cases. Application of the Siegert pseudostates may require introduction of the hyperspherical coordinates [34]. The ECS Hamiltonian can be directly diagonalized in a multidimensional space providing nuclear states with the outgoing-wave boundary condition in each of the dissociative coordinates.

#### ACKNOWLEDGMENTS

The work of C.H.G. has been supported by the U.S. Department of Energy, Office of Science, under Grant No. DE-SC0010545, Basic Energy Sciences. R.Č. acknowledges support of the Czech Science Foundation (Grant No. GACR 18-02098S). The work of D.H. was supported by the Czech Science Foundation (Grant No. GACR P203/17-26751Y).

- 
- [1] E. S. Chang and U. Fano, *Phys. Rev. A* **6**, 173 (1972).  
 [2] D. M. Chase, *Phys. Rev.* **104**, 838 (1956).  
 [3] M. A. Morrison and W. Sun, in *Computational Methods for Electron-Molecule Collisions*, 1st ed. edited by W. M. Hue and F. A. Gianturco (Plenum, New York, 1995), Chap. 6, p. 170.  
 [4] M. Cascella, R. Čurík, F. Gianturco, and N. Sanna, *J. Chem. Phys.* **114**, 1989 (2001).  
 [5] R. Čurík and F. A. Gianturco, *J. Phys. B: At. Mol. Opt. Phys.* **35**, 1235 (2002).  
 [6] M. J. Seaton, *Rep. Prog. Phys.* **46**, 167 (1983).  
 [7] M. Aymar, C. H. Greene, and E. Luc-Koenig, *Rev. Mod. Phys.* **68**, 1015 (1996).  
 [8] C. Jungen and D. Dill, *J. Chem. Phys.* **73**, 3338 (1980).  
 [9] C. Jungen, *Phys. Rev. Lett.* **53**, 2394 (1984).  
 [10] C. H. Greene and C. Jungen, *Advances in Atomic and Molecular Physics* (Academic, Orlando, Florida, 1985), Vol. 21, pp. 51–121.  
 [11] E. L. Hamilton and C. H. Greene, *Phys. Rev. Lett.* **89**, 263003 (2002).  
 [12] H. Takagi, *Phys. Rev. A* **70**, 022709 (2004).  
 [13] R. Čurík and C. H. Greene, *Phys. Rev. Lett.* **98**, 173201 (2007).  
 [14] R. Čurík and C. H. Greene, *J. Chem. Phys.* **147**, 054307 (2017).  
 [15] M. Ayouz and V. Kokoouline, *Atoms* **4**, 30 (2016).  
 [16] M. Khamesian, M. Ayouz, J. Singh, and V. Kokoouline, *Atoms* **6**, 49 (2018).  
 [17] V. Kokoouline and C. H. Greene, *Phys. Rev. A* **68**, 012703 (2003).  
 [18] C. H. Greene and C. Jungen, *Phys. Rev. Lett.* **55**, 1066 (1985).  
 [19] H. Gao and C. Greene, *J. Chem. Phys.* **91**, 3988 (1989).  
 [20] F. Robicheaux, *Phys. Rev. A* **43**, 5946 (1991).  
 [21] H. Gao and C. H. Greene, *Phys. Rev. A* **42**, 6946 (1990).  
 [22] D. Hvizdoš, M. Váňa, K. Houfek, C. H. Greene, T. N. Rescigno, C. W. McCurdy, and R. Čurík, *Phys. Rev. A* **97**, 022704 (2018).  
 [23] R. Čurík, D. Hvizdoš, and C. H. Greene, *Phys. Rev. A* **98**, 062706 (2018).  
 [24] C. M. Lee, *Phys. Rev. A* **10**, 584 (1974).  
 [25] R. Čurík and C. H. Greene, *Mol. Phys.* **105**, 1565 (2007).  
 [26] R. Čurík and F. A. Gianturco, *Phys. Rev. A* **87**, 012705 (2013).  
 [27] A. J. F. Siegert, *Phys. Rep.* **56**, 750 (1939).  
 [28] O. I. Tolstikhin, V. N. Ostrovsky, and H. Nakamura, *Phys. Rev. Lett.* **79**, 2026 (1997).  
 [29] O. I. Tolstikhin, V. N. Ostrovsky, and H. Nakamura, *Phys. Rev. A* **58**, 2077 (1998).  
 [30] B. Simon, *Phys. Lett. A* **71**, 211 (1979).  
 [31] C. W. McCurdy and F. Martín, *J. Phys. B: At., Mol. Opt. Phys.* **37**, 917 (2004).  
 [32] A. Giusti, *J. Phys. B: At., Mol. Phys.* **13**, 3867 (1980).  
 [33] F. O. Waffeu Tamo, H. Buhr, O. Motapon, S. Altevogt, V. M. Andrianarijaona, M. Grieser, L. Lammich, M. Lestinsky, M. Motsch, I. Nevo *et al.*, *Phys. Rev. A* **84**, 022710 (2011).  
 [34] V. Kokoouline and C. H. Greene, *Phys. Rev. Lett.* **90**, 133201 (2003).